

Research report

Interaction between discrete and rhythmic movements: reaction time and phase of discrete movement initiation during oscillatory movements

Aymar de Rugy*, Dagmar Sternad

Department of Kinesiology, The Pennsylvania State University, 266 Recreation Building, University Park, PA 16802, USA

Accepted 16 September 2003

Abstract

This study investigates a task in which discrete and rhythmic movements are combined in a single-joint elbow rotation. Previous studies reported a tendency for the EMG burst associated with the discrete movement to occur around the expected burst associated with the rhythmic movement (e.g., [Exp. Brain Res. 99 (1994) 325; J. Neurol. Neurosurg. Psychiatry 40 (1977) 1129; Hum. Mov. Sci. 19 (2000) 627]). We document this interaction between discrete and rhythmic movements in different task variations and suggest a model consisting of rhythmic and discrete pattern generators that reproduces the major results. In the experiment, subjects performed single-joint elbow oscillatory movements (2 Hz). Upon a signal, they initiated a movement that consisted of a shift in the midpoint of the oscillation (MID), a shift in the amplitude of the oscillation (AMP), or a combination of both (MID + AMP). These shifting movements were performed either in a reaction time or in a self-paced fashion. The tendency for the EMG bursts associated with the discrete and rhythmic movements to synchronize was found similarly in all three tasks and instruction conditions, but the synchronization was most pronounced in the self-initiated discrete movement. Reaction time was increased for the combined task (MID + AMP), indicating higher control demands due to a combination of discrete and rhythmic components. This EMG burst synchronization was reproduced in a model based on a half-center oscillator with activation signals that produce either rhythmic or discrete activity. This activity was interpreted as torques driving a simple limb model. Summation of discrete and rhythmic activation signals of the pattern generators was sufficient to simulate the EMG burst synchronization. Further, simulation data reproduced the modulation of the reaction time as a function of the phase of the discrete movement. © 2003 Elsevier B.V. All rights reserved.

Theme: G

Topic: Control of posture and movement

Keywords: Reaction time; Rhythmic movements; Discrete movements; Pattern generator

1. Introduction

Continuous rhythmic actions, such as walking or running, and discrete actions, such as reaching, represent two important classes of movements. Numerous studies on movement control and coordination have addressed either one or the other type of movement. However, more complex actions and new challenges for coordination may come from the combination of both types of actions. Everyday behaviors are full of examples of such combinations. Reaching out to shake someone's hand while walking is one such combination. The complex trajectories of cursive handwriting

provide another good example as they have been modeled both as a sequence of discrete strokes [37] or as a coupling of oscillations [14,16]. More likely, they may be considered as a complex parallel and sequential combination of both types of "movement primitives". In previous work on single-limb, inter-, and intra-limb coordination, we have argued that discrete and rhythmic movements are two fundamental units of action governed by two different control regimes that can be combined into more complex actions [25,26,33,35,38]. A similar distinction into continuously rhythmic and discrete tasks has been supported in studies on cerebellar patients that show selected deficits in tasks with discrete temporal or spatial targets [28] and split-brain patients [17]. Differences in the rhythmic and discrete performance of a Fitts-type task have led to the same conclusion on two types of primitives [4,27]. The focus of the present study is on single-joint movements engaged in

* Corresponding author. Tel.: +1-814-863-0355; fax: +1-814-865-1275.

E-mail address: aug3@psu.edu (A. de Rugy).

different types of action sequences of discrete and rhythmic elements with a specific focus on the constraints between the two movement elements.

While the first studies on voluntary human movements performed on the background of rhythmic movements were on tremor (e.g., Refs. [17,36]), more recent work also examined voluntary rhythmic and discrete movement combinations. A central and robust result in all these experiments is that the initiation of the discrete movement is constrained by the rhythmic cycle. For example Hallet et al. [13] revealed in a study on Parkinson patients that the EMG bursts associated with the production of a discrete movement occurred at approximately the same points in time that EMG activity would have been expected if tremor oscillations were simply continuing (see also Refs. [30,39]). We will refer to this effect as “EMG burst synchronization”, i.e., the timing of the discrete burst tends to synchronize with the rhythmic burst. Important for the understanding of complex voluntary movements is that this effect was also found in discrete movements performed against the background of voluntary slower rhythmic movement between 2 and 7 Hz [2,31,34]. In recent studies, we further showed that this EMG burst synchronization occurs irrespective of the frequency of the rhythmic movement [34], and of the mechanical load added to the moving limb [38]. Similar constraints were also shown to matter in multijoint and bimanual coordination [33,38].

In order to explain this EMG burst synchronization effect, Staude et al. [29–31] proposed a model for the interaction between discrete and rhythmic movements. This model is based on a threshold mechanism that operates on the superposed control signals for the rhythmic and the discrete movements. Using simple sinusoidal and ramp-like signals the model simulated the constrained distribution of onset phases of the discrete movement. Sternad et al. [34] suggested a model that consists of two pattern generators for both rhythmic and discrete movements, which included reciprocal coupling between the discrete and rhythmic movement components. While reproducing some features of the kinematic trajectories, the mechanism that inhibits the discrete pattern generator produced data that were not entirely consistent with empirical results. With the objective to resolve this discrepancy, the present experiment was designed to provide experimental data with further task variations. On the basis of new results a model will be developed that is based on the notion of neural pattern generators for rhythmic and discrete movements coupled to a biomechanical limb.

Besides the phase of the discrete initiation, another important aspect of the interaction between discrete and rhythmic movements is the reaction time of the discrete movement. If the discrete onset is constrained to a certain phase window of the ongoing rhythmic movement—even if the discrete movement is to be performed as fast as possible after the pseudo-randomized trigger signal—reaction time is necessarily modulated. Experimental results

with respect to reaction time, however, have been contradictory. In the case of tremor, Lakie and Combes [18] did not report an effect on the reaction time. For voluntary discrete movements, Sternad et al. [34] failed to discern systematic variations in reaction time in conjunction with the observed phase onset effect. Conversely, Michaels and Bongers [23] and Latash [20] reported that reaction time depended on the phase of the ongoing oscillation. This effect was greater when reaction time was related to the phase of the response than when it was related to the phase of the stimulus. Neither of these studies, however, provided further explanation for this finding. Moreover, both studies focused on reaction time only, disregarding the phase onset of the discrete movement with respect to the rhythmic movement. As a consequence, the expected link between the two features was left unaddressed. In contrast, Staude et al. [31] addressed this issue. However, in their analysis of experimental and simulated data, they assumed that the interaction between discrete and rhythmic movement can only produce delays in the onsets of the discrete movement, and not advances, as suggested by the study of Latash [20]. Therefore, the first objective of the present study is to provide data to clarify this issue and suggest a model that encompasses both the EMG-burst synchronization and the reaction time modulation.

The fact that the onset of the discrete movement is confined to a phase window of the rhythmic movement, even if the task is to produce a discrete movement as soon as possible after a trigger signal, highlights the strength of this effect. If this tendency for EMG burst synchronization is a physiological constraint, then the onset should be even more tightly clustered at the virtual rhythmic burst if the timing constraints are relaxed and the subject can choose the moment of discrete initiation. For subjects with physiological tremor [10] and Parkinson disease [39], as well as for voluntary movements in three healthy subjects [2], however, a comparison between a time-stressed and a self-paced instruction did not identify differences. Extending from these unexpected results, the second main interest of the present study is to compare self-paced with time-stressed performance.

The third and last purpose of the present study is to compare different combinations of discrete and rhythmic movements. Specifically, three tasks were designed that involved a discrete shift in the midpoint of the oscillation (MID), an increase in the amplitude of the oscillation (AMP), or a combination of both (MID+AMP) (Fig. 1). While the task MID was the one used in many previous studies [2,29,31,34,35], the tasks AMP and MID+AMP include changes in movement amplitude, a parameter of the rhythmic movement. Assuming two different control regimes for rhythmic and discrete movements, the task MID involved a rhythmic movement combined with a discrete movement. The task AMP involved only a reparameterization of the oscillation. Furthermore, the task MID+AMP required changing two movement parameters.

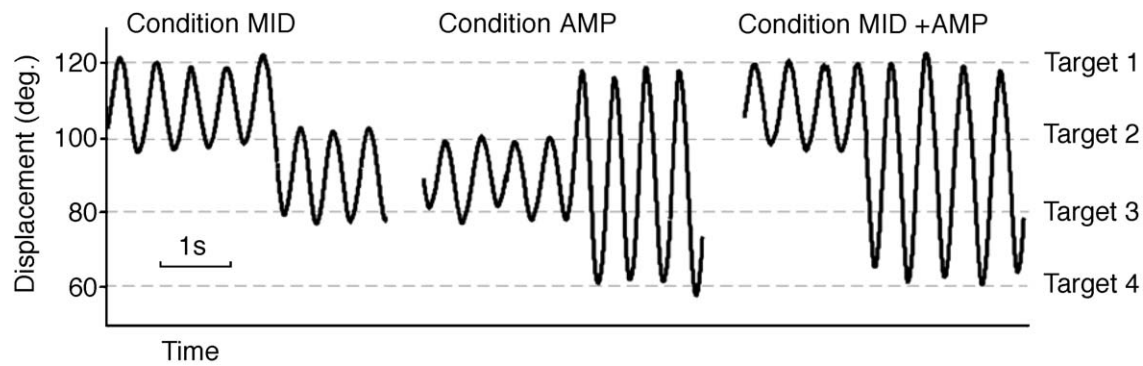


Fig. 1. Representative trial segments as an illustration of the three movements conditions.

Following this conception, MID+AMP constituted the most complex task and longer reaction times are expected.

2. Method

2.1. Subjects

Six graduate students and faculty members (five male, one female) from The Pennsylvania State University volunteered to be subjects in this study. Their ages ranged from 20 to 43 years. All reported themselves to be right-hand dominant and none reported any history of serious injury to their right arms. The subjects were informed about the experimental procedure and subsequently signed the consent form in agreement with the University's Regulatory Committee.

2.2. Experimental apparatus and data collection

The subject was seated in front of a table with his/her right forearm placed on a padded horizontal metal support affixed to a vertical axle around which it rotated. The height of the chair was adjusted so that the arm was horizontal and at the same height as the forearm. The center of rotation of the elbow joint was aligned with the axle of the apparatus. Because the chest rested against the table, shoulder movements were minimized and elbow flexion and extension occurred in the horizontal plane. The shoulder angle, measured between the line between the two shoulders and the upper arm, was approximately 150° . There were small differences in this angle between subjects due to anatomical differences. This angle was not precisely controlled and resulted from subjects resting their chest against the edge of the table. The subjects grasped a vertical wooden handle affixed to the end of the forearm support with their right hand. To ensure a fixed forearm position on the support, the forearm rested in a plastic brace and a Velcro band was strapped moderately tightly around the forearm support. Targets were created on a vertical cardboard surface curved in the horizontal plane, which was placed such that the distance between the curved path of the tips of the fingers

and the target surface was 5 cm. Four targets indicated elbow angles of 120° , 100° , 80° , and 60° for targets 1, 2, 3 and 4, respectively. A computer-generated metronome signaled the oscillation periods for an initial pacing (beep duration: 50 ms, beep frequency: 2500 Hz). After the initial pacing interval, a single tone (200 ms, 4000 Hz) served as the stimulus to signal the onset of the discrete movement.

Joint angle position data were collected by a potentiometer affixed to the axle of the apparatus. Measurement resolution of this device was 1° . Electromyographic data was collected from one elbow flexor, the long head of the biceps brachii (BB), and one elbow extensor, the lateral head of the triceps (TL) by means of surface electrodes. As forearm and arm were positioned horizontally in the basic experimental posture, the influence of gravity on the movements was minimal, so that the primary functions of the measured muscles were flexion and extension. The EMG signal was analog highpass filtered (10 Hz) and lowpass filtered (1000 Hz) and amplified with a gain of 5 K. The sampling frequency for both EMG and elbow position was 500 Hz. (This sampling frequency was sufficient as the unfiltered signal did not contain frequencies higher than 250 Hz, bypassing aliasing effects). In addition to the EMG and kinematic signals, the auditory signal was recorded to provide information about the temporal onset of the stimuli. The collection of all signals was controlled by LabView Software (National Instruments, Austin, TX) on a Macintosh Computer (PowerCenter Pro 210, Power Computing).

2.3. Experimental conditions

The subject was instructed to oscillate his/her forearm between two visible targets in synchrony with the auditory metronome, performing one full cycle per beep. The metronome period was set to 2 Hz for all conditions. The subject was instructed to coordinate maximum flexion excursions with the metronome beeps. After 5 s, the metronome signal terminated but the subject was instructed to continue oscillating at the same frequency until he/she heard another trigger signal. This stimulus tone occurred after a delay of between 2 and 5 s after cessation of the initial pacing interval. The duration of this delay was

specified by the output of a pseudorandom number generator. The subject was instructed that upon hearing this tone, he/she was to oscillate between the two new targets.

Three movement conditions were presented. Fig. 1 illustrates the three task conditions with three representative trials. In condition 1 (MID), the subject was required to first oscillate between Targets 1 and 2 (120° and 100°), and after the trigger signal to oscillate between Targets 2 and 3 (100° and 80°). This instruction implied a shift in the midpoint of the oscillation (from 110° to 90°). In condition 2 (AMP), the subject was required to first oscillate between Targets 2 and 3 (100° and 80°) and then to oscillate between Targets 1 and 4 (120° and 60°). This implied a change in the amplitude of the oscillation (from a 20° to a 60° amplitude). In condition 3 (MID + AMP), the subject first oscillated between Targets 1 and 2 and then between Targets 1 and 4. This movement involved both a shift in the midpoint of the oscillation, as in condition MID, from 110° to 90° , and a change in the amplitude of the oscillation, as in condition AMP, from 20° to 60° amplitude. No explicit performance feedback was given, but subjects were instructed to match the movement amplitudes to the targets relying on their perception of the visual correspondence between their hand and targets. Fig. 1 illustrates that subjects matched the target amplitudes sufficiently well.

These three task conditions were performed under two timing instructions. The first, termed “reaction time” (RT), required the subject to react as fast as possible. More specifically, the subject was instructed to “reach the new targets of the oscillatory movement as fast as possible after the signal”. For condition MID, Target 3 should be reached as fast as possible. In contrast, for condition AMP, it was either Target 1 or Target 4 that could be reached as fast as possible. For condition MID + AMP, it was Target 4. The instruction emphasized that both the reaction time to the signal and the speed of the change should be as fast as possible. The second timing instruction, termed “self-paced” (SP), allowed the subject to initiate the change in the oscillatory movement whenever he/she felt most comfortable after the trigger signal. When he/she decided to initiate the new oscillatory movement, however, the subject was required to perform the change as fast as possible. In sum, the combination of the three movement conditions with two timing instructions gave a total of six experimental conditions.

A practice session comprising two trials per condition, presented randomly, was given to familiarize subjects with the different experimental conditions. Fifteen trials of each condition were performed by each subject where the temporal onset of the trigger signal was randomly distributed across oscillatory phases. The assumption was that the onsets of the trigger signal were uniformly distributed across the oscillatory cycle. The six sessions of 15 trials were performed in a block-design. The order of the blocks was randomized for each participant. The duration of the entire experimental session was approximately 45 min.

2.4. Data reduction and analysis

The digitized EMG signals were rectified and filtered using a sixth-order low-pass Butterworth filter with a cut-off frequency of 35 Hz. The joint angle signals measured by the potentiometer were low-pass filtered at 20 Hz. For both muscles, the timing of each activity burst during the rhythmic movement was calculated. To this end, the EMG signals were divided into windows where each window contained one EMG burst. The window boundaries were defined by the joint angle excursions. The maxima of the elbow flexion proved to be the best separator for BB and the maxima of extension delineated the EMG signal of the TL (for an exemplary trial with an elbow flexion in condition MID see Fig. 2). Within each window, the time of peak activity of the burst was determined by the center of mass (COM) of the EMG signal within each window. To obtain the COM of an EMG burst, the area under the rectified EMG curve within each window was calculated using the trapezoidal method of numerical integration. The time of the COM, t_{COM} , was then identified as the half-area point of the EMG signal within each window. If the discrete action was executed as a flexion movement (oscillatory condition MID and MID + AMP, and part of the trials of condition AMP), the EMG signal of the biceps was analyzed. Conversely, if the discrete action was made with an extension movement (part of the trials of condition AMP), the EMG signal of the triceps was analyzed. Posthoc visual evaluation showed that the COM proved to be a robust representation of peak activity in the EMG signal and was a more reliable estimate than single maxima.

The onset of the discrete movement was determined in two ways. First, the onset of the discrete burst's activity, t_{onset} , was determined by using a threshold. Second, the time of the discrete movement, t_{disc} , was determined as the time of the COM of the burst responsible for the discrete movement. The first estimate t_{onset} relies on a threshold that defines the onset of the discrete burst. Although such a threshold measure has been used in all previous studies, it is problematic as it is heavily dependent on a somewhat arbitrarily chosen threshold. Yet, in order to compare the results of this study with previous findings (e.g., Refs. [25–29,31]), the onset of the discrete EMG burst was calculated using a threshold algorithm taken from Abbink et al. [1]. This method suggests a statistical criterion for a non-interactive onset detection in rhythmic EMG signals. To determine the threshold delimiting significant burst activity, a histogram of the entire EMG signal is calculated first. For rhythmic signals this histogram of EMG amplitudes is Gaussian-like and amplitudes that pertain to significant burst activity are defined to be larger than $\mu + 3\sigma$, where μ corresponds to the mean and σ to the standard deviations of the fitted normal distribution to the histogram. This threshold was applied to determine the time of discrete burst's onset t_{onset} .

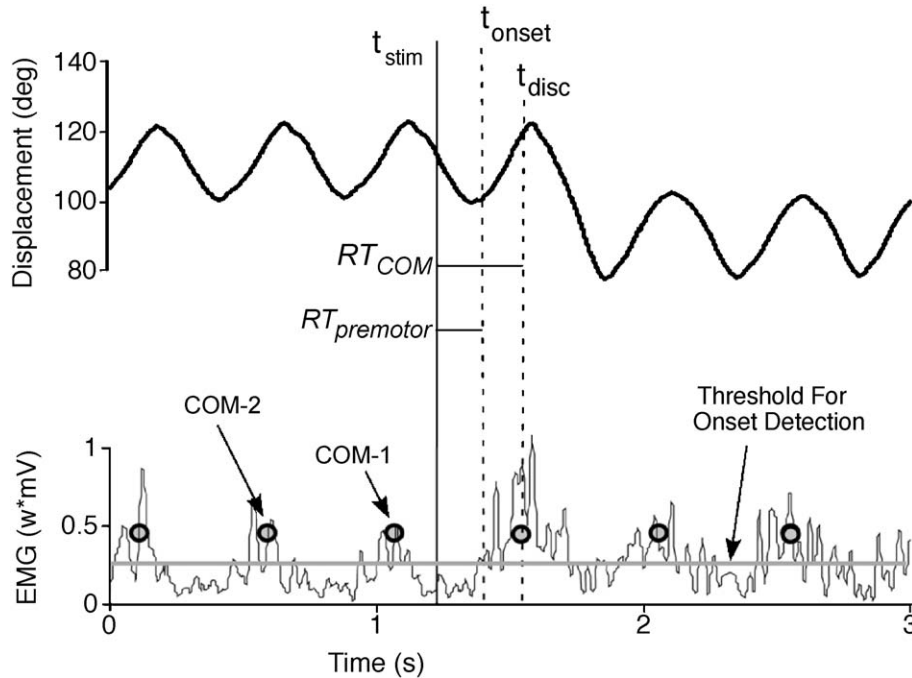


Fig. 2. A segment of a representative time series. The onset and the center of mass (COM) of the discrete movement are illustrated (t_{onset} and t_{disc}). Black circles correspond to the COM of EMG bursts.

The phases of t_{onset} and t_{disc} relative to the rhythmic bursts associated with the oscillation, ϕ_{onset} and ϕ_{disc} , were calculated according to:

$$\phi_{\text{onset}} = 2\pi \frac{t_{\text{onset}} - t_{\text{COM-1}}}{T} \bmod 2\pi \quad \text{and} \quad (4)$$

$$\phi_{\text{disc}} = 2\pi \frac{t_{\text{disc}} - t_{\text{COM-1}}}{T} \bmod 2\pi$$

where $t_{\text{COM-1}}$ refers to the time of the COM of the burst one cycle before the discrete onset. T is the average period of five cycles preceding the discrete movement and $t_{\text{COM-1}}$ is the time of the COM of the EMG burst one cycle before the discrete burst. Hence, phase 0 rad is defined at the moment of peak activity of each rhythmic burst in the EMG signals.

Reaction time in the trials with “reaction time” instruction was also estimated in two ways: First, RT_{premotor} was defined as the difference between t_{stim} and t_{onset} , as is common for the calculation of premotor reaction time. Second, based on the COM, RT_{COM} was defined as the difference between the auditory stimulus t_{stim} and t_{disc} (see Fig. 2). For further analysis, RT_{COM} values that were not in the range between 100 and 600 ms were excluded. This only occurred in six trials. For RT_{premotor} a larger number of unrealistic values were obtained that were mostly too short. As we wanted to avoid introducing an arbitrary threshold, all data were included. For the data obtained with the “self-paced” instruction, an equivalent measure was calculated, i.e., the time between t_{stim} and t_{disc} , but was called signal-to-onset time (ST), as it is meaningless to speak of reaction time. Indeed, the subjects were required to perform the discrete movement whenever they felt most comfortable

after t_{stim} which sometimes occurred several cycles after t_{stim} . Despite this, ST still remained a valuable variable to consider as will be seen in the results below.

To quantify how RT_{COM} of the discrete movement was modulated by the rhythmic movement, we first defined the “expected onset” of the discrete movement as t_{stim} plus the average reaction time $\overline{RT}_{\text{COM}}$ calculated for each subject over the 15 trials obtained for each combination of instruction and movement conditions. Note that these calculations were only performed for RT_{COM} as RT_{premotor} did not give sufficiently reliable results. By adding $\overline{RT}_{\text{COM}}$ to t_{stim} , we thus obtained the time and phase where the onset would have occurred in the absence of the phasic influence of the oscillation. The expected phase with respect to the rhythmic movement ϕ_{exp} was defined as follows:

$$\phi_{\text{exp}} = 2\pi \frac{(t_{\text{stim}} + \overline{RT}_{\text{COM}}) - t_{\text{COM-1}}}{T} \bmod 2\pi \quad (5)$$

For further analysis $\overline{RT}_{\text{COM}}$ was normalized as subjects showed different mean reaction times. Hence, the difference between the actual RT_{COM} and $\overline{RT}_{\text{COM}}$, obtained for each subject in the reaction time instruction, was calculated as follows:

$$RT_{\text{norm}} = RT_{\text{COM}} - \overline{RT}_{\text{COM}} \quad (6)$$

RT_{norm} refers to normalized reaction time. Correspondingly, ST_{norm} was calculated as the difference between the actual and the mean signal-to-onset time \overline{ST} .

The distributions of ϕ_{disc} and ϕ_{onset} were compared between the experimental conditions as well as related to

the simulated phase onsets by means of χ^2 analysis. A mixed-design two-way ANOVA (task \times subject) was conducted on RT_{COM} and $RT_{premotor}$ values obtained in each trial of the “reaction time” (RT) instruction condition.

3. Results

3.1. Phase onset of the discrete movement

Since the reliability of calculation of phase measures depended on the constancy of the cycle periods T preceding the discrete movement, the variability of the cycle periods calculated over the intervals of five cycles with and without the metronome was compared. A global t -test on the standard deviations of periods calculated for the five cycles preceding the discrete movement and for the last five cycles performed with the metronome did not detect a statistical difference. These standard deviations were 20 and 21 ms, respectively. Hence, the calculation of ϕ_{onset} , ϕ_{disc} , and ϕ_{exp} was regarded to be sufficiently reliable.

Fig. 3 represents the distributions of the phase of the onset of the discrete movement ϕ_{onset} for the three task conditions MID, AMP, and MID+AMP, each performed under one of the two timing instructions “reaction time” RT and “self-paced” SP. All six figures show that ϕ_{onset} most frequently occurred at approximately $3\pi/2$ rad and least often between 0 and π rad. χ^2 tests established that all distributions were significantly different from a uniform

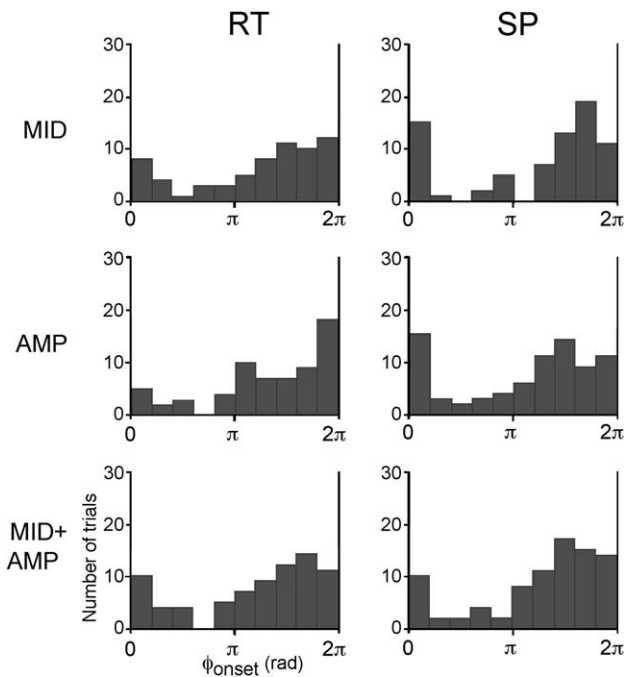


Fig. 3. Distributions of the phase of the onset of the discrete movement ϕ_{onset} for the three movement conditions MID, AMP, and MID+AMP and for the two timing instructions, RT for “reaction time” condition, and SP for the “self-paced” condition.

Table 1

χ^2 values for the pairwise comparisons of the distributions of the phase of the EMG onset of the discrete movement, ϕ_{onset} , and of the COM of the discrete movement, ϕ_{disc} , obtained in the RT (reaction time) and the SP (self-paced) instruction

	RT versus Uniform		SP versus Uniform		RT versus SP	
	ϕ_{onset}	ϕ_{disc}	ϕ_{onset}	ϕ_{disc}	ϕ_{onset}	ϕ_{disc}
Condition MID	33.59*	66.39*	60.22*	188.33*	28.28*	59.03*
Condition AMP	35.33*	75.74*	25.86*	122.21*	18.11	46.69*
Condition MID+AMP	31.11*	42.83*	40.44*	137.9*	8.08	33.11*

Comparisons with a uniform distribution, and with each other are reported. The asterisk indicates statistically significant differences ($\alpha < 0.01$).

distribution ($\alpha < 0.01$). RT and SP conditions differed only for the MID task. Comparisons between the ϕ_{onset} distributions obtained in the different task conditions within either the RT or the SP instructions revealed only one significant difference between the distributions obtained in conditions MID and AMP under the SP instruction. These results are summarized in Tables 1 and 2.

Fig. 4 shows the distributions of the phase of the COM of the discrete movement ϕ_{disc} for every experimental condition. Visual inspection shows that the patterns are more pronounced than for ϕ_{onset} . Moreover, the distributions are shifted by approximately 1/4 cycle. All six figures show that ϕ_{disc} occurred mostly around a phase of 0 rad, or equivalently 2π rad, and rarely at a phase of π rad, which corresponded to the midpoint between two expected rhythmic bursts. χ^2 tests established that all distributions were significantly different from a uniform distribution ($\alpha < 0.01$). As the results in Table 1 show, these values were considerably higher than the ones obtained for ϕ_{onset} . Furthermore, the figure shows that this constraint on the onset was visibly more pronounced in the SP than in the RT instruction. Pairwise χ^2 comparisons between the RT and SP distributions were performed for all three task conditions and yielded significant differences. Table 2 presents the χ^2 results from the comparisons between the ϕ_{disc} distributions obtained in the different task conditions within either the RT or the SP instruction. Only one significant difference was found between the distributions obtained in conditions MID and AMP under the RT instruction, but was associated with a relatively small χ^2 value. None of the other distributions obtained within the RT or the SP instructions could be

Table 2

χ^2 values of the comparisons the distributions of ϕ_{onset} and of ϕ_{disc} between the different movement conditions

	RT		SP	
	ϕ_{onset}	ϕ_{disc}	ϕ_{onset}	ϕ_{disc}
MID versus AMP	20.28	28.04*	28.75*	9.02
MID versus MID+AMP	10.56	14.42	21.70	6.31
AMP versus MID+AMP	18.69	16.98	9.65	3.35

Pairwise comparisons were performed within both the RT (reaction time) or the SP (self-paced) instruction. The asterisk indicates statistically significant differences ($\alpha = 0.01$).

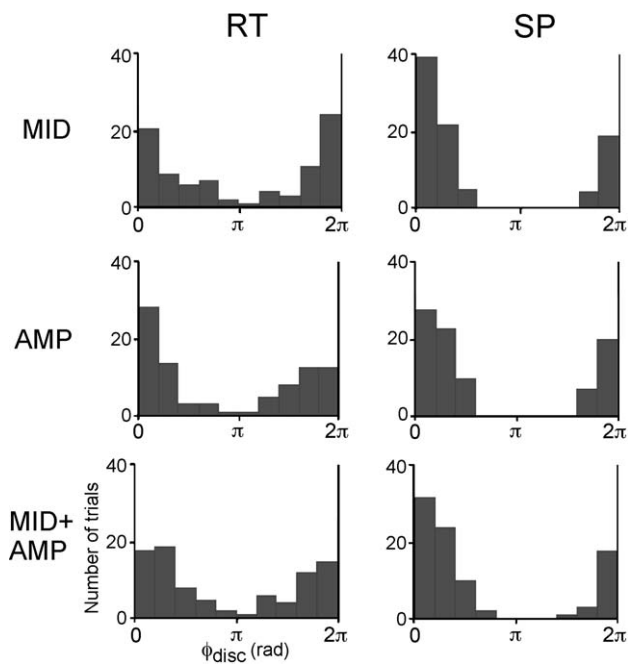


Fig. 4. Distributions of the phase of the COM of the discrete movement ϕ_{disc} for the three movement conditions MID, AMP, and MID+AMP and for the two timing instructions, RT for “reaction time” condition, and SP for the “self-paced” condition.

distinguished. In sum, the fact that ϕ_{disc} occurred at 0 or 2π rad indicated that the two bursts were synchronized. The pattern of results was more pronounced for ϕ_{disc} .

As explained in Methods, for each subject a virtual or expected onset phase ϕ_{exp} was also computed. When plotting the observed ϕ_{disc} against ϕ_{exp} , the modulation of this actual onset became clear. Fig. 5 shows the data for the two SP and RT instructions, respectively. For the uniformly distributed ϕ_{exp} , the observed ϕ_{disc} were highly clustered. Fig. 5-RT shows that for ϕ_{exp} close to 0 and 2π rad, ϕ_{disc} values were confined to 0 or 2π rad. The closer ϕ_{exp} was to π rad, the weaker this effect became. For the SP instruction, this effect was even more extreme (Fig. 5-SP). When ϕ_{onset} was plotted in the same fashion against ϕ_{exp} , however, the pattern disappeared almost completely. Together with the less systematic results in the distributions of ϕ_{onset} compared to ϕ_{disc} , this finding demonstrates that the phase measure based on the center of EMG activity COM was considerably better in revealing the phase-dependent effects on the execution of the discrete movement.

3.2. Reaction time

In order to test the effect of task on reaction time, a task \times subject ANOVA was performed on $\text{RT}_{\text{premotor}}$ values. The analysis rendered significant main effects for task, $F(2, 140) = 3.90$, $p < 0.05$, and subject, $F(5, 140) = 5.95$, $p < 0.05$, as well as an interaction between task and subject, $F(10, 140) = 4.49$, $p < 0.05$. The shortest $\text{RT}_{\text{premotor}}$ values were found in condition AMP with an average of 162 ms;

condition MID had a mean $\text{RT}_{\text{premotor}}$ of 183 ms, and for MID+AMP it was 212 ms. Posthoc pairwise Tukey tests identified only the difference between AMP and MID+AMP as significant. These results, however, need to be interpreted with caution. Fig. 6A illustrates the distribution of $\text{RT}_{\text{premotor}}$ for the RT instruction. As can be seen, small estimates for $\text{RT}_{\text{premotor}}$ and for several trials even negative $\text{RT}_{\text{premotor}}$ values were obtained using the onset detection algorithm. The threshold was clearly too low, and led to false onset detections. If the threshold was increased, however, the opposite problem arose and onsets were missed. No threshold could be identified that eliminated both too short reaction time values or missed onsets. One important problem linked to a proper threshold determination was that the width and amplitude of the discrete bursts were dependent on the amplitude of the discrete movement. As different amplitudes were involved in the experimental conditions, the onset would be defined on different grounds for the three conditions.

Rather than adjusting the threshold “by eye” for unrealistic picks, we opted to calculate reaction time on the basis of

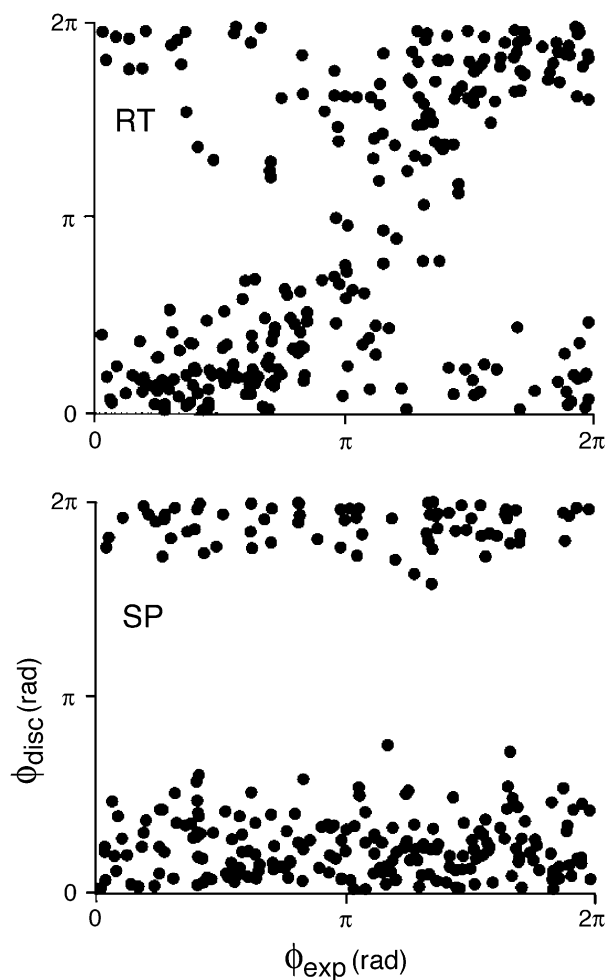


Fig. 5. Observed onset phase of the discrete movement ϕ_{disc} plotted against the expected onset phase ϕ_{exp} for the two instruction conditions RT and SP.

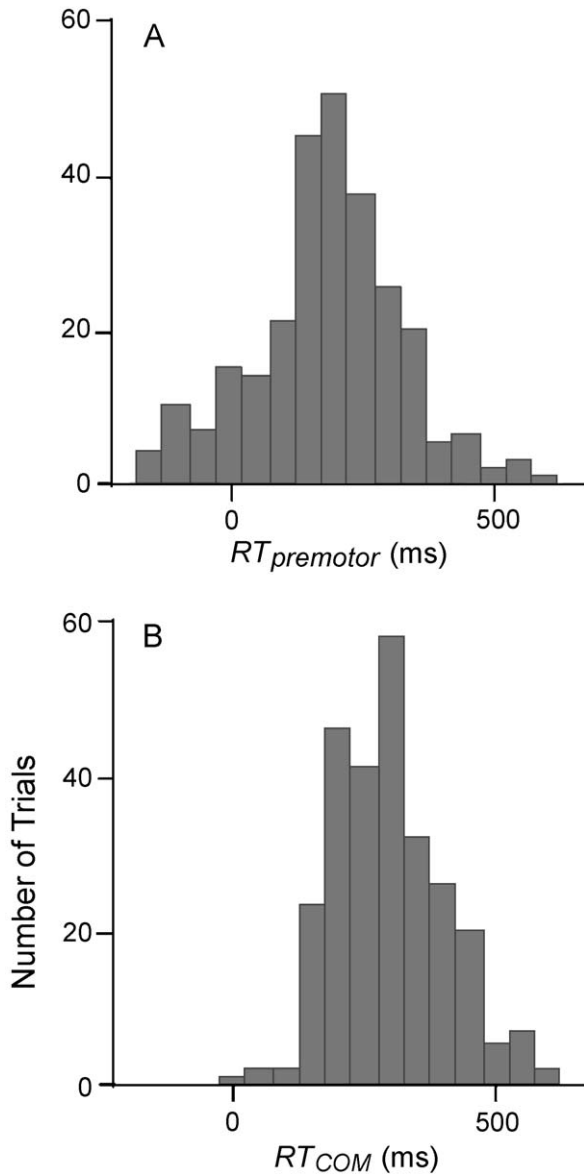


Fig. 6. Distributions of the reaction times obtained for the “reaction time” condition, calculated from the threshold based onset detection ($RT_{premotor}$) (A) and from the COM of the discrete burst (RT_{COM}) (B).

the center of mass of the discrete burst. As already implied in the previous results, the COM proved a reliable estimate for characterizing rhythmic activity and was independent of kinematic variations. The distribution of RT_{COM} is shown in Fig. 6B. With the exception of six trials where RT_{COM} was below 100 ms, all other values were regarded as realistic.

Performing the same ANOVA with RT_{COM} as the dependent measure, significant main effects were obtained for task, $F(2, 140) = 8.08, p < 0.05$, and subject, $F(5, 140) = 2.86, p < 0.05$, as well as an interaction between task and subject, $F(10, 140) = 3.09, p < 0.05$. The longest RT_{COM} was found in condition MID + AMP with an average of 330 ms, condition AMP had a mean value of 290 ms, and MID had the shortest RT_{COM} of 275 ms over the five subjects. Posthoc pairwise

Tukey tests identified differences between MID and MID + AMP and between AMP and MID + AMP as significant. Averages and variability of RT_{COM} are presented in Table 3 for every subject and every experimental condition.

To contrast the reaction time values with ST, the ST values of all subjects are also shown in Table 3. The same mixed-design two-way ANOVA revealed a significant main effect for subject, $F(5, 140) = 19.43, p < 0.05$, as well as an interaction between task and subject, $F(10, 140) = 6.72, p < 0.05$, but no significant effect for task.

As subjects showed differences in the average RT_{COM} , RT_{COM} s were normalized by subtracting the subject averages (RT_{norm}), so that the data of all subjects could be pooled for further analysis. To examine the dependency of reaction time on the phase of the rhythmic movement, RT_{norm} was plotted as a function of the phase that would have been expected with a constant reaction time, ϕ_{exp} . Fig. 7-RT displays the RT_{norm} of all subjects’ trials pooled and plotted as a function of ϕ_{exp} . For the RT instruction, RT_{norm} were shorter than average for trials where ϕ_{exp} ranged between 0 and π rad, and RT_{norm} were longer than average for ϕ_{exp} between π and 2π rad. Within each half-cycle, the data clustered in an approximately linear fashion with ϕ_{exp} and changed discontinuously by one cycle period (500 ms) to the second cluster of data. This means that when the COM would have occurred between two expected bursts associated with the rhythmic movement, subjects either shortened or lengthened their RT_{COM} in order to synchronize the discrete burst with one of the ongoing rhythmic bursts. This point will be further clarified when the model for EMG burst synchronization will be proposed. No differences in this pattern were observed for the different task conditions.

This pattern is even more pronounced for the SP instruction shown in Fig. 7-SP. ST_{norm} was found to scale monotonically with ϕ_{exp} . The two streams of data clouds were separated by one period of the oscillation. This meant that subjects sometimes waited for one, or sometimes even for two full cycles to initiate the discrete movement. The large

Table 3

Means and standard deviation (in parentheses) of reaction time (RT_{COM}) and signal-to-onset time (ST) are presented for each subject as a function of instruction and movement condition (MID, AMP, MID + AMP)

	RT_{COM}			ST		
	MID	AMP	MID + AMP	MID	AMP	MID + AMP
S1	244 (82)	280 (63)	306 (127)	637 (277)	561 (175)	541 (308)
S2	290 (111)	328 (127)	363 (87)	773 (223)	798 (199)	943 (198)
S3	271 (82)	307 (109)	286 (80)	808 (154)	414 (127)	757 (157)
S4	236 (64)	297 (122)	292 (119)	412 (184)	362 (127)	462 (138)
S5	308 (103)	292 (91)	331 (51)	472 (272)	664 (243)	624 (198)
S6	302 (116)	232 (64)	402 (106)	550 (261)	789 (294)	617 (130)
S	275 (93)	290 (96)	330 (95)	608 (229)	598 (194)	657 (188)

Values are reported in millisecond. The last line presents the values averaged over the six subjects (S).

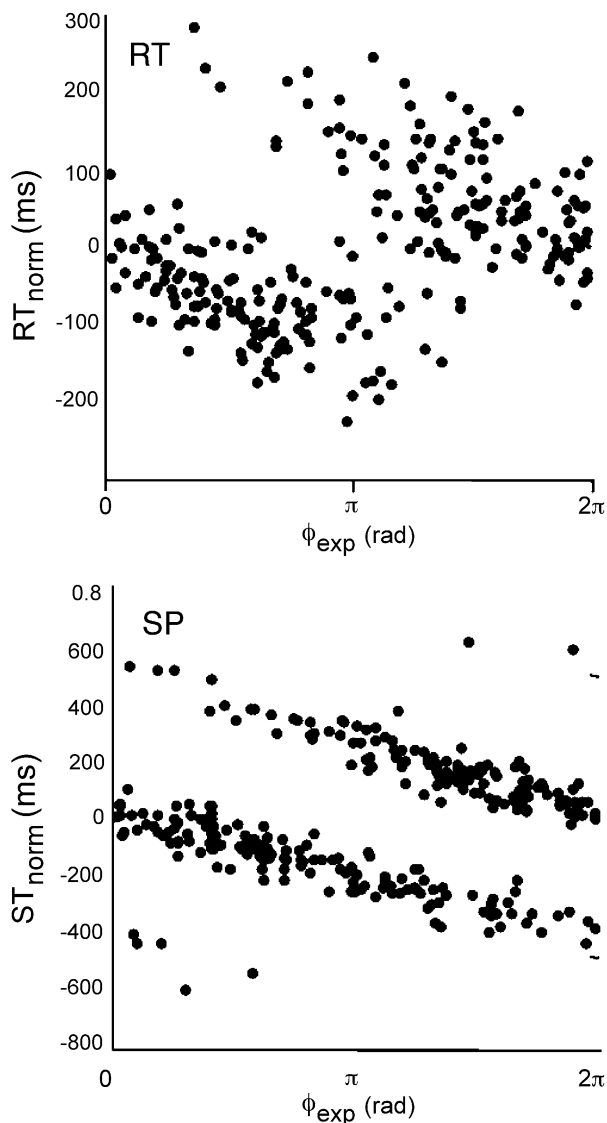


Fig. 7. Reaction time modulation as a function of the phase of the expected onset for both the “reaction time” (RT) and the “self-paced” (SP) instruction.

negative values around -500 ms were due to the fact that average ST was relatively high. These data points do not indicate premature initiations.

4. Discussion

Several previous studies reported that when discrete and rhythmic movements are performed simultaneously, the initiation of the discrete movement is restricted to a specific phase window of the oscillatory motion [2,8,10,13,29–31,34–36,38,39]. All studies that focused their analyses on EMG activity agreed that the main EMG burst associated with the discrete movement occurred preferentially around the same time or approximately 1/4 cycle before an EMG burst would have been expected, if the rhythmic movements

were simply continuing (e.g., Refs. [13,36]). Some studies also measured premotor reaction times of the discrete initiation but inconsistent results were reported [2,18,20,23,31,34]. The main interest of the present study was to get more clarification about the nature of the interaction between discrete and rhythmic components in single-joint voluntary movements and propose a model that accounts for the observed effects.

We extended previous work by including three different task variations that involved a discrete shift in the midpoint of the oscillation (MID), an increase in the amplitude of the oscillation (AMP), or a combination of both (MID+AMP). Providing that the task AMP may be viewed as a reparameterization of the oscillation rather than a separate discrete movement, we asked whether a similar synchronization effect was to be found in this task. Furthermore, since the task MID+AMP required a change both in the discrete and in the rhythmic component of the movement, the higher demands of this task should be reflected in longer reaction times.

Assuming that a physiological constraint is responsible for this interaction, we hypothesized that this constraint will be affected by varying the instruction. When the subject is allowed to freely initiate the discrete movement and combine it with the ongoing oscillation in a preferred fashion, he/she will choose the moment that is physiologically optimal. In contrast, when the discrete movement is to be initiated as fast as possible following a trigger signal given at a random phase of the oscillation, then this intention may reveal the limits set by the physiological constraints. Therefore, our experiment involved subjects performing a discrete movement against the background of voluntary movements under two timing instructions: self-paced and reaction time.

4.1. Experimental results

The results on the initiation constraints of the discrete movement were replicated in all three tasks showing that discrete and rhythmic components cannot be combined arbitrarily when the same antagonistic muscles are shared. The histograms of the phases of the discrete activity in all six experimental conditions showed the similar characteristic that performing a discrete movement was limited to the phase where the oscillation activity would have occurred. It is worth noting that this phenomenon is much more pronounced for measures calculated with the COM of the discrete burst rather than its onset. This blurring of the pattern may be due to the errors induced by the threshold-based onset detection. More importantly, though, this result suggests that it is the center of rhythmic EMG activity that entrains the discrete burst, rather than a threshold that limits the activation of discrete burst activity to certain phases. Also, in all conditions there is a consistent shift in phase by 1/4 cycle in the histogram’s mode depending on whether phase was determined with a threshold or with the center of mass. The COM-based calculations, revealing synchroniza-

tion in phase with the rhythmic burst, strongly suggest a synchronization mechanism. This will be made explicit in the model suggested below.

The comparison between the two instructions showed that for the self-paced initiation, this initiation constraint was more pronounced than for the reaction time condition. This difference was not found in earlier studies on tremor [10,39]. However, it would not be surprising if such small differences were beyond the resolution that experimental measurements can reveal in the high-frequency signals of tremor. Similar negative results were reported by Adamovich et al. [2] for voluntary movements, but the authors did not report any quantitative results. The comparison between the three task conditions only revealed a difference between the discrete phase distributions of the MID and AMP movement conditions in the “fast” instruction. However, this effect was relatively small, and was even absent when the conditions MID or AMP were compared with the condition MID+AMP. Thus, the effects of the interaction between discrete and rhythmic movements appeared similar, regardless whether the discrete action consisted of a shift in the midpoint of the rhythmic movement, a shift in the amplitude of the rhythmic movement, or a combination of both. A common mechanism responsible for synchronization in EMG bursts will be illustrated with the model below.

Turning to reaction time, the first analyses of premotor reaction time showed that despite the problems due to the threshold determination, the subject averages were higher than the typical simple premotor reaction times that are reported for discrete tasks without the simultaneous rhythmic movement. The overall average in the present data was 175 ms, even though many unrealistically small values were included. For instance Nakamura and Saito [24] reported an average of 137 ms for simple premotor reaction time to an auditory signal performed by an elbow movement. This is consistent with Michaels and Bongers [23] who also reported slower reaction times for discrete movements performed on the background of rhythmic activity. It remains that Latash [20] observed that at certain phases of the rhythmic movement, premotor reaction times could drop even below the level seen without the rhythmic movement (180 ms for visual stimuli). This difference in results is probably due to the fact that in the present experiment and in Michaels and Bongers’ study the oscillations were to be maintained and oriented to specific targets, while in Latash’s study the oscillations could be discontinued with the initiation of the discrete movement. Due to the threshold problems of the onset detection algorithm, the reaction times calculated on the basis of the center of mass were more reliable for further interpretation. Further, the width and amplitude of the discrete bursts are dependent on the amplitude of the discrete movement. As different amplitudes were involved in the experimental conditions, the onset would be defined on different grounds for the three conditions. Hence, a criterion based on the center of mass appears to be more consistent.

Comparison of RT_{COM} across the three tasks and subjects showed that RT_{COM} was significantly longer in MID+AMP. While this was also seen as a trend in premotor reaction time, the results were considerably clearer across subjects in RT_{COM} . This effect is noteworthy because the kinematic pattern at the moment of initiation does not show a difference between the three tasks. Hence, consistent with our hypothesis that led to the design of the tasks, this increased RT_{COM} probably reflects higher control demands as the MID+AMP task involved both the initiation of a second discrete regime and the reparameterization of the rhythmic regime.

Looking at normalized reaction times, there was a consistent pattern such that shorter RT_{norm} were found for ϕ_{exp} between 0 and π rad, and longer RT_{norm} for ϕ_{exp} between π and 2π rad. This is consistent with the EMG burst synchronization shown in Fig. 4: Expected discrete onsets close to peak EMG activity at 0 rad get shortened to occur earlier, and onsets that occur between π and 2π rad get prolonged to coincide with the next rhythmic EMG burst at 2π rad. It should be emphasized that the mean, RT_{COM} , or zero RT_{norm} , was obtained by averaging over all delayed and advanced reaction times. So, while RT_{COM} was advanced, it can only be said that it was shorter than the average RT_{COM} for this task.

In the following section, we will suggest a model that accounts for both observations on phase onset and reaction time.

4.2. Model for EMG burst synchronization

In order to account for the interactions between discrete and rhythmic movements, we propose a model that was developed using the concept of half-center oscillators. In continuation of previous work, we suggest that discrete and rhythmic movements are two types of control regimes governed by pattern generators. Each pattern generator activates a muscle synergy that consists of an antagonistic pair of muscles [7,34]. Depending on the activation signal, the pattern generator produces either a discrete displacement or a rhythmic movement. In the case of a single-degree-of-freedom movement as in the present experiment, where a combination of rhythmic and discrete movements is involved, a single synergy is assumed to execute the movement. It consists of two interconnected neuronal pools for two antagonistic muscles that are driven by the two pattern generators. The output of the pattern generators is interpreted as muscular activation that generates torques acting at the elbow joint, thereby generating joint angle trajectories. In the following development, we show that a simple model of a neural oscillator can produce patterns of muscular activation similar to both rhythmic and discrete movements. Furthermore, when the inputs for discrete and rhythmic movements are summed, the observed EMG burst synchronization emerges from the dynamics of the pattern generators.

The oscillatory pattern generator was developed by Matsuoka [21,22] and expresses the basic mechanism of a

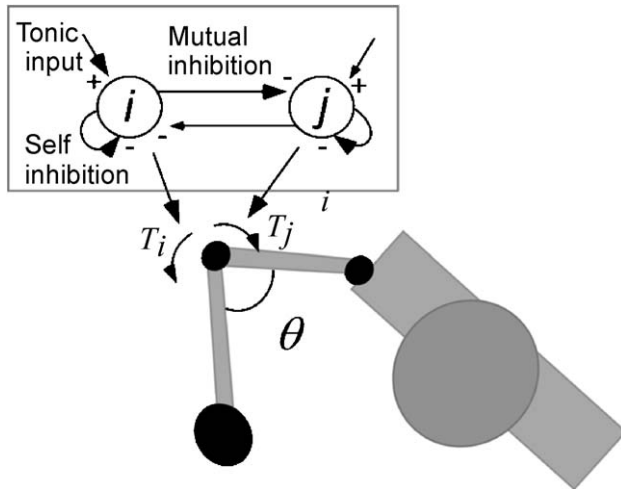


Fig. 8. Illustration of the model for EMG burst synchronization tendency. The neural oscillator drives the mechanical limb by generating alternating torques at the elbow joint.

half-center oscillator. It consists of two neurons, i and j , each of whose activity is generated by the following equations:

$$\begin{aligned} t_1 \dot{\psi}_i &= -\psi_i + s_R - b\varphi_i - w[\psi_j]^+ \\ t_2 \dot{\varphi}_i &= -\varphi_i + [\psi_i]^+ \end{aligned} \quad (6)$$

where ψ_i represents the firing rate of neuron i , and φ_i governs its self-inhibition. Each neuron receives the tonic

input s_R , and inhibits the other through $-w[\psi_j]^+$ (see Fig. 8). The bracket notation expresses that only positive values are considered and the term is zero if the argument is negative. w is the gain for this coupling term and b is the gain for the self-inhibition. t_1 and t_2 are two time constants. The same equations govern the activity of neuron j .

The oscillator controls the activity of two antagonistic “muscles” i and j operating at the elbow (Fig. 8). Their output is interpreted as opposing torques that are a linear function of the output of each neuronal unit:

$$T_i = h_T[\psi_i]^+ \quad (7)$$

$$T_j = -h_T[\psi_j]^+$$

where h_T is the gain of the torques. In the following simulations, h_T was set to 5. Angular displacement of the forearm θ is generated by the inertial system driven by the imbalance between the two torques:

$$I\ddot{\theta} + \gamma\dot{\theta} - (T_i + T_j) = 0 \quad (8)$$

I is the moment of inertia of the forearm plus racket and γ is the damping of the elbow. The values for I and γ were taken from the literature that measured human rhythmic elbow movements: $\gamma = 0.5$ Nm/rad/s; $I = 0.08$ Nm/rad/s² [3].

When each neuron receives the tonic input s_R , the output of the Matsuoka oscillator displays bursts of the units i and j which alternate (Fig. 9A). Considering only the positive

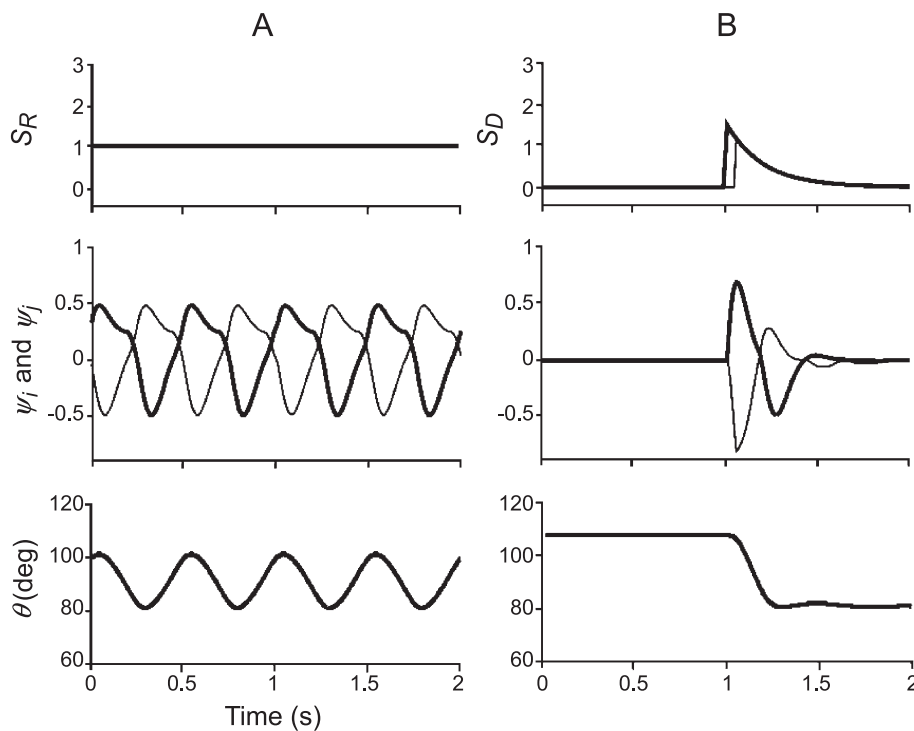


Fig. 9. Simulation of rhythmic and discrete movement. (A) The neural oscillator receives a tonic input s_R and produces an output (ψ_i and ψ_j) consisting of alternating. The positive parts of ψ_i and ψ_j are interpreted as the alternating EMG bursts responsible for the rhythmic movement. (B) The neural oscillator receives a phasic input s_D and produces a triphasic output pattern that generates the discrete movement of the limb.

parts, the output of the neural oscillator can be interpreted as the alternating EMG bursts responsible for rhythmic movement. These bursts drive the forearm, which generate the rhythmic kinematic signal θ . The parameters of the simulation for Fig. 9A were $s_R=1$; $b=2.5$; $w=2.5$, $t_1=0.05$, and $t_2=0.125$. Fig. 9B shows how a discrete movement can be generated by the same pattern generator if the activation signal is different. When the same pair of half-center units receives a phasic input s_D , the typical triphasic pattern of bursts is observed as known for single discrete movements (e.g. [32]). The signal s_D is generated by a pulse followed by an exponential decay:

$$t_3 \dot{s}_D = -s_D + s_{D0} \quad (9)$$

where t_3 is the time constant of the first-order dynamics, and s_{D0} is the initial value of s_D at t_0 , which is the time of the discrete change in the activation signal. Note that unit i receives the discrete input at t_0 , while unit j receives it a short time later (50 ms). This small difference is necessary such that unit i “wins” to create the intended “flexion” burst. Fig. 9B illustrates the phasic input s_D as well as the resulting triphasic pattern of activation. The lowest panel illustrates the kinematic signal that shows the typical angular displacement θ with a small overshoot or even oscillatory approach to the target position. The simulation for Fig. 9B was run with $t_3=0.2$ and $s_{D0}=1.5$.

The next objective is to combine s_R and s_D to simulate the experimental tasks consisting of both rhythmic and discrete elements. Fig. 10 illustrates the resulting patterns. To reproduce the condition MID, a discrete shift in the oscillation midpoint is generated at t_0 by the sum of s_R and s_D . Linear unweighted summation is regarded as the first simple way to account for the coexistence of two input signals (see also Ref. [31]). This combined input s_{RD} is sent to the same neural oscillator. The small circles in unit i

(shown in bold) denote the COM of the burst that was determined with the same algorithm using the kinematic output as for the experimental data. The two circles in the larger burst indicate that this burst produces the discrete movement. To simulate the condition AMP, the change in the amplitude of the oscillation is obtained by resetting s_R to a higher value at t_0 (from $s_{RD}=1$ to $s_{RD}=3$). To simulate the condition MID+AMP, s_D was added at the same time t_0 as when s_R was changed. Both s_D and s_R were identical to the ones used for the simulations of MID and AMP, respectively. In all three conditions, the unit j receives the change in s_R 50 ms later than the unit i . The reason for this time lag is to ascertain that the “flexor” unit i wins as for MID and AMP+MID subjects were instructed to perform a flexion in the discrete movement. For AMP, it was observed that subjects tended to prefer one unit to initiate the increase in the amplitude.

Note that the patterns show qualitative agreement with the intended pattern in some ways but also deviate in other ways (Fig. 1). While MID is reproduced in sufficient qualitative and quantitative agreement with the real kinematic trajectories, both AMP and MID+AMP deviate from the intended pattern. In AMP, the amplitude is increased as intended, but the midpoint of oscillation is also shifted more than subjects performed. Similarly in MID+AMP, the midpoint for the second part is shifted too much. However, the quantitative change in the amplitude corresponds well to the one seen in the subjects’ data. To better control the accuracy of the midpoint shift, an additional mechanism has to be included as will be discussed further below. However, as the emphasis of this paper is on the reaction time and phase of onset, we refrain from further refinement of the model at this point.

Turning to the major experimental results of reaction time and phase of the discrete onset, simulations were run to

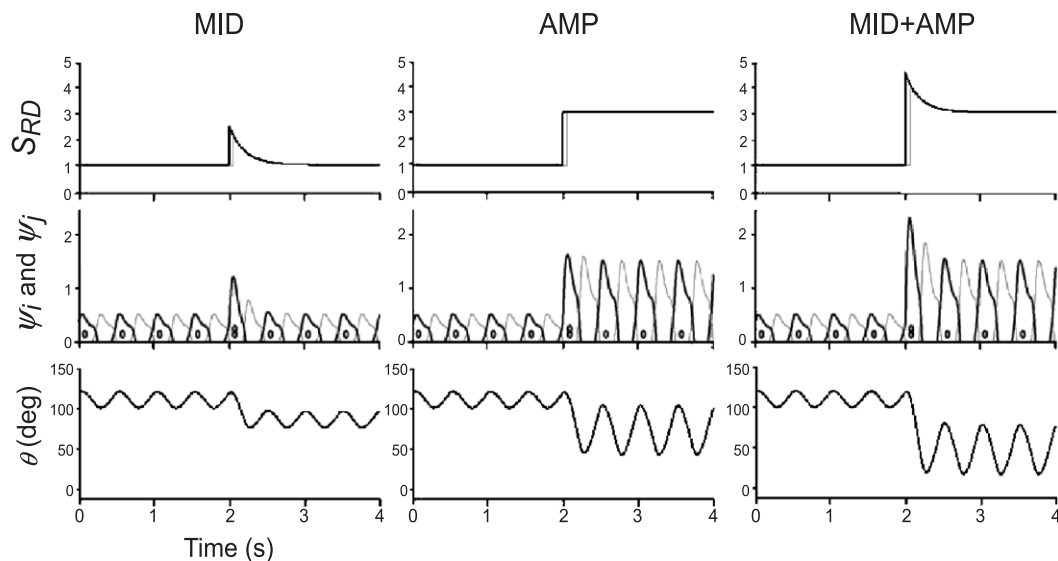


Fig. 10. Simulation of the three movement conditions (MID, AMP and MID+AMP). Input (s_{RD}) and output (ψ_i and ψ_j) of the neural oscillator are presented together with the resulting angular displacement θ .

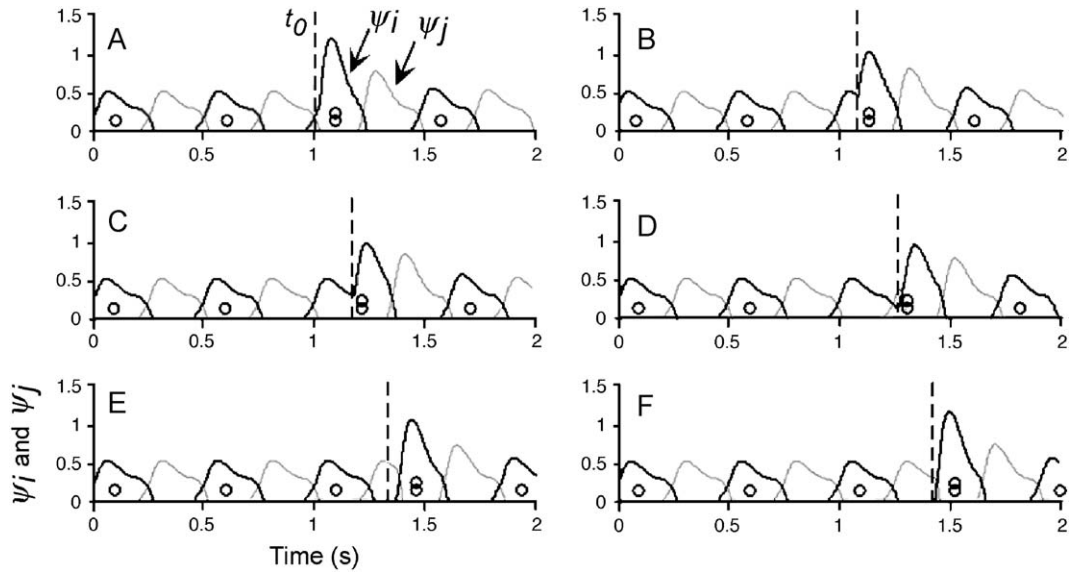


Fig. 11. Simulated output of the Matsuoka pattern generator (ψ_i and ψ_j) for condition MID with six different t_0 of the summed input s_{RD} . From panels A to F, t_0 was increased to span one rhythmic cycle across two bursts of units i .

test whether the observed EMG burst synchronization can emerge from this model. To illustrate the underlying mechanism, Fig. 11 shows the simulated output of the pattern generators ψ_i and ψ_j for condition MID with six different t_0 and thereby phase of the summed input s_{RD} . Panels A to F show simulations for six different t_0 , equivalent to six onset phases across one rhythmic cycle of unit i . The bold lines refer to unit i that performs the intended flexion movement. The small circles in the bursts refer to the COMs calculated for the bursts of unit i with the same algorithm as used for the experimental data. Two circles demarcate the burst that produces the discrete movement. Fig. 11A shows that an onset of t_0 at the beginning of unit i , i.e., at ϕ_{exp} close to 0 rad, leads to an amplification of the rhythmic burst to produce the discrete movement. When t_0 occurs later during the rhythmic burst, i.e., ϕ_{exp} is closer to π rad, this burst becomes broader and shows two peaks but still remains one connected burst (Fig. 11B–D). As the COM is determined across the entire broadened burst, the computed reaction times are shorter. When t_0 occurs after π rad, as in Fig. 11E, excitation of unit i occurs when unit i is inhibited by unit j . Hence, the activation is delayed until the subsequent burst and reaction time becomes longer. ϕ_{disc} is closer to 2π rad than ϕ_{exp} . If t_0 occurs even later, as in Fig. 11F, an amplification of the subsequent rhythmic burst occurs similar to as in Fig. 11A.

Fig. 12 shows the results of the analysis of 200 simulations per condition, each run with a different t_0 uniformly distributed across one cycle. These simulated data were analyzed in the same way as in the experiment to determine ϕ_{disc} and ϕ_{exp} . The reaction times were calculated as the time between t_0 and the COM associated with the burst responsible for the discrete movement. Fig. 12 presents the distributions of ϕ_{disc} (left), as well as RT_{COM} as a function

of ϕ_{exp} (right). The distributions of ϕ_{disc} showed similar patterns as the experimental data where the least number of bursts occurred around π rad in favor of 0 and 2π rad. Furthermore, when plotting RT_{COM} as a function of ϕ_{exp} , a qualitatively similar modulation as in the experiment was obtained: RT_{COM} was shorter for ϕ_{exp} between 0 and π rad, and longer between π and 2π rad with a relatively abrupt change close to π rad. These simulated results are qualitatively similar for the three movements condition, despite

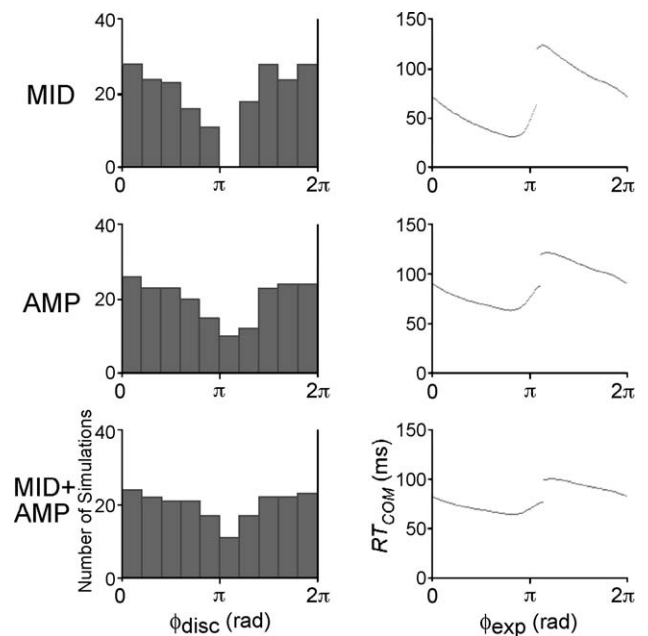


Fig. 12. Distributions of ϕ_{disc} and reaction time plotted as a function of ϕ_{exp} for 200 simulations run for different timing of the discrete input within two expected rhythmic bursts, for MID, AMP, and MID+AMP.

differences in the magnitude of the effect. In sum, the patterns are in agreement with the ones found in the data and replicate the EMG burst synchronization and the results of ϕ_{disc} and RT_{COM} that follow from it.

The model is an extension of previous theoretical and experimental work [25,33–35,38]. More specifically, the present model builds on the concept of Central Pattern Generators (CPGs) as mutually inhibiting neural units that produce alternating activation of antagonistic muscles. This concept has received support in the context of animal and human locomotion (e.g., Refs. [5,6,11]), and was more recently applied to explain human upper limb rhythmic movements (e.g., Ref. [12]). With the current model, we propose that the concept of a CPG can be generalized to not only produce rhythmic but also discrete movements. With this compatible formulation, it is possible to address the combined control of rhythmic and discrete movement components. Due to the sharing of the same circuitry and basic connectivity, we can simulate the identified synchronization tendency for rhythmic and discrete bursts. In contrast, Sternad et al. [34] had developed a model that consisted of two coupled pattern generators, one for the rhythmic and one for the discrete movement. These two pattern generators were different in their structure and were coupled by a mutual inhibition. This inhibitory coupling, however, suppressed the discrete initiation during (rhythmic) activity of the antagonistic unit and thereby could only produce delays in the initiation of the discrete movement and not advances. Therefore, the distribution of the simulated onset data showed a marked asymmetry, counter to the symmetrical distribution around the mode between $3\pi/2$ and 2π rad in the data. These discrepancies were the major motivation that the current revision of the model aimed to resolve. It was clear that an inhibition with a threshold mechanism could not account for the symmetrically distributed data. Further, the previous analyses of reaction time were unable to extract systematic patterns. This was probably due to the fact that the calculations relied on threshold detection and also that the notion of expected phase was not introduced. In sum, the fact that the current analysis defined the dependent measures on the basis of the center of mass, and thereby introduced the notion of EMG burst synchronization, resolved many facets of the data.

In a series of studies, Staude et al. [29–31] also developed a model for the interaction between rhythmic and discrete signals. The model proposes a threshold mechanism that operates on the algebraic summation of two independent control signals for the discrete and rhythmic movements and other feedback signals. While the rhythmic signal is a sine function, the signal for the discrete movement is a ramp. A threshold function that acts on the sum of the two signals determines the onset of the discrete movement. In addition to the methodological problem of identifying this onset on a background of rhythmic activity, their model can only produce phase delays. As pointed out above, the present data and model aim to argue that the underlying

mechanism is rather a tendency for synchronization of two bursts within a single effector rather than a threshold mechanism.

One additional new component in the current model is the inclusion of limb dynamics, admittedly in a very simplified fashion. This produces “kinematic” data so that the model output can be similarly analyzed as the experimental data. However, this component also highlights a shortcoming of the current model. As pointed out in Fig. 10, the proposed minimal system is unable to locate the trajectory at targets in extrinsic space. In a more general sense the present model does not possess stability properties at the level of the kinematics, such that any perturbation remains uncompensated. As such, this model is incomplete and requires further development to include stability features associated with position in extrinsic space. Several possibilities exist, ranging from different combinations of feed-forward and feedback mechanisms (e.g., Ref. [15]) to the framework of the equilibrium point hypothesis (e.g., Refs. [9,19]). An elaboration of this feature, however, is beyond the scope of the current study which focused on EMG burst activity and its mechanisms to produce phase synchronization and reaction time modulation. Despite this shortcoming, we believe that the model illustrates and maybe even explains the mechanism responsible for the observed effects.

In conclusion, insights into the interaction of rhythmic and discrete movements can be relevant to understand movement pathologies. It highlights that pronounced tremor limits the initiation of new movements to phases of the tremor cycle. Further, complex skills such as handwriting may be subject to the same constraints as identified here. In the example of cursive handwriting, invoked in Introduction, the pen moves up and down in a quasi-oscillatory fashion but directed discrete strokes for new letters have to be inserted at certain phases. It is likely that similar constraints as the ones identified in the present experimental task may determine features of the pen's trajectory.

Acknowledgements

This research was supported by the National Science Foundation, Behavioral Neuroscience #00-96543.

References

- [1] J.H. Abbink, A. van der Bilt, H.W. van der Glas, Detection of onset and termination of muscle activity in surface electromyograms, *J. Oral Rehabil.* 25 (1998) 365–369.
- [2] S.V. Adamovich, M.F. Levin, A.G. Feldman, Merging different motor patterns: coordination between rhythmical and discrete single-joint movements, *Exp. Brain Res.* 99 (1994) 325–337.
- [3] J. Bennett, J.M. Hollerbach, Y. Xu, I.W. Hunter, Time-varying stiffness of voluntary elbow joint during cyclic voluntary movement, *Exp. Brain Res.* 88 (1992) 433–442.
- [4] J.J. Buchanan, J.H. Park, Y.U. Ryu, C.H. Shea, Discrete and cyclical units of action in a mixed target pair aiming task, *Exp. Brain Res.* 50 (2003) 473–489.

- [5] B. Bussel, A. Roby-Bramie, O. Rémi-Néris, A. Yakovlevff, Evidence for a spinal stepping generator in man, *Paraplegia* 34 (1996) 91–92.
- [6] B. Calancie, B. Needham-Shropshire, P. Jacobs, K. Willer, G. Zych, B.A. Green, Involuntary stepping after chronic spinal cord injury. Evidence for a central rhythm generator for locomotion in man, *Brain* 117 (1994) 1143–1159.
- [7] A. de Rugy, K. Wei, H., Müller, D. Sternad, Actively tracking “passive” stability in a ball bouncing task. *Brain Res.* (accepted).
- [8] R.J. Elble, C. Higgins, L. Hughes, Essential tremor entrains rapid voluntary movements, *Exp. Neurol.* 126 (1994) 138–143.
- [9] A.G. Feldman, Once more on the equilibrium-point hypothesis (λ model) for motor control, *J. Mot. Behav.* 18 (1986) 17–54.
- [10] D. Goodman, J.A.S. Kelso, Exploring the functional significance of physiological tremor: a biospectroscopic approach, *Exp. Brain Res.* 49 (1983) 419–431.
- [11] S. Grillner, Neurobiological bases of rhythmic motor acts in vertebrates, *Science* 228 (1985) 143–149.
- [12] S. Grossberg, C. Pribe, C., M.A. Cohen, Neural control of interlimb oscillations: I. Human bimanual coordinations, *Biol. Cybern.* 77 (1997) 131–140.
- [13] M. Hallet, B.T. Shahani, R.R. Young, Analysis of stereotyped voluntary movements at the elbow in patients with Parkinson disease, *J. Neurol. Neurosurg. Psych.* 40 (1977) 1129–1135.
- [14] J.M. Hollerbach, An oscillation theory of handwriting, *Biol. Cybern.* 39 (1981) 139–156.
- [15] M.I. Jordan, D.E. Rumelhart, Forward models: supervising learning with a distal teacher, *Cogn. Sci.* 16 (1992) 307–354.
- [16] K.-T. Kalveram, A neural oscillator model learning given trajectories, or how an “allo-imitation algorithm” can be implemented into a motor controller, in: J. Piek (Ed.), *Motor Behavior and Human Skill, Human Kinetics, Champaign, 1998*, pp. 127–140.
- [17] S.W. Kennerley, J. Diedrichsen, E. Hazeltine, A. Semjen, R.B. Ivry, Callosotomy patients exhibit temporal uncoupling during continuous bimanual movements, *Nat. Neurosci.* 5 (2002) 718–730.
- [18] M. Lakie, N. Combes, There is no simple temporal relationship between the initiation of rapid reactive hand movements and the phase of an enhanced physiological tremor in man, *J. Physiol.* 523 (2000) 515–522.
- [19] M.L. Latash, Virtual trajectories, joint stiffness, and changes in the limb natural frequency during single-joint oscillatory movements, *Neuroscience* 49 (1992) 209–220.
- [20] M.L. Latash, Modulation of simple reaction time on the background of an oscillatory action: implications for synergy organization, *Exp. Brain Res.* 131 (2000) 85–100.
- [21] K. Matsuoka, Sustained oscillations generated by mutually inhibiting neurons with adaptation, *Biol. Cybern.* 52 (1985) 367–376.
- [22] K. Matsuoka, Mechanisms of frequency and pattern control in the neural rhythm generators, *Biol. Cybern.* 56 (1987) 345–353.
- [23] C.F. Michaels, R.M. Bongers, The dependence of discrete movements on rhythmic movements: simple RT during oscillatory tracking, *Hum. Mov. Sci.* 13 (1994) 473–493.
- [24] R. Nakamura, H. Saito, Preferred hand and reaction time in different movement patterns, *Percept. Mot. Skills* 39 (1974) 1275–1281.
- [25] S. Schaal, D. Sternad, R. Osu, M. Kawato, Rhythmic movement is not discrete. 31st Annual Meeting of the Society for Neuroscience, San Diego, 2001 (November 10–15).
- [26] S. Schaal, D. Sternad, R. Osu, M. Kawato, Rhythmic movements are not discrete. *Nat. Neurosci.* (submitted).
- [27] B.C.M. Smits-Engelsman, G.P. Van Galen, J. Duysens, The breakdown of Fitts’ law in rapid, reciprocal aiming movements, *Exp. Brain Res.* 145 (2002) 222–230.
- [28] R.M. Spencer, H.N. Zelaznik, J. Diedrichsen, R.B. Ivry, Disrupted timing of discontinuous but not continuous movements by cerebellar lesions, *Science* 300 (2003) 1437–1439.
- [29] G. Staud, W. Wolf, Quantitative assessment of phase entrainment between discrete and cyclic motor actions, *Biomed. Tech.* 42 (1997) 478–481.
- [30] G. Staud, W. Wolf, M. Ott, W.H. Oertel, R. Dengler, Tremor as a factor in prolonged reaction times of Parkinsonian patients, *Mov. Disord.* 10 (1995) 153–162.
- [31] G. Staud, R. Dengler, W. Wolf, The discontinuous nature of motor execution: II. Merging discrete and rhythmic movements in a single-joint system—the phase entrainment effect, *Biol. Cybern.* 86 (2002) 427–443.
- [32] D. Sternad, D. Corcos, Effect of task and instruction on patterns of muscle activation: Wachholder and beyond, *Mot. Control* 5 (2001) 307–336.
- [33] D. Sternad, W.J. Dean, Rhythmic and discrete elements in multijoint coordination. *Brain Res.* (in press).
- [34] D. Sternad, W.J. Dean, S. Schaal, Interaction of rhythmic and discrete pattern generators in single-joint movements, *Hum. Mov. Sci.* 19 (2000) 627–664.
- [35] D. Sternad, A. de Rugy, T. Pataky, W. Dean, Interaction of discrete and rhythmic movements over a wide range of periods, *Exp. Brain Res.* 147 (2002) 162–174.
- [36] L.E. Travis, The relation of voluntary movement to tremors, *J. Exp. Psych.* 12 (1929) 515–524.
- [37] P. Viviani, C. Terzuolo, Trajectory determines movement dynamics, *Neuroscience* 7 (1982) 431–437.
- [38] K. Wei, G. Wertman, D. Sternad, Interactions between rhythmic and discrete components in a bimanual task, *Mot. Control* 7 (2003) 134–155.
- [39] M.M. Wierzbicka, G. Staud, W. Wolf, R. Dengler, Relationship between tremor and the onset of rapid voluntary contraction in Parkinson’s disease, *J. Neurosurg. Psych.* 56 (1993) 782–787.